Journal of Hazardous Materials 187 (2011) 407–412

Contents lists available at ScienceDirect

Journal of Hazardous Materials

journal homepage: www.elsevier.com/locate/jhazmat

Toxic pollutants emitted from thermal decomposition of phthalimide compounds

Kai Chen, John C. Mackie[1], Dominika Wojtalewicz, Eric M. Kennedy, Bogdan Z. Dlugogorski*

Process Safety and Environmental Protection Research Group, School of Engineering, The University of Newcastle, Callaghan, New South Wales 2308, Australia

ARTICLE INFO

Article history:
Received 3 December 2010
Accepted 11 January 2011
Available online 15 January 2011

Keywords:
Phthalimide compounds
Air pollutants
Dibenzo-*p*-dioxin
Dibenzofuran

ABSTRACT

Phthalimide (PI) and tetrahydrophthalimide (THPI) are two structurally similar compounds extensively used as intermediates for the synthesis of variety of industrial chemicals. This paper investigates the thermal decomposition of PI and THPI under oxygen rich to oxygen lean conditions, quantifying the production of toxicants and explaining their formation pathways. The experiments involved a plug flow reactor followed by silica cartridges, activated charcoal trap and a condenser, with the decomposition products identified and quantified by Fourier transform infrared spectroscopy (FTIR), gas chromatography–mass spectrometry (GC–MS) and micro gas chromatography (μGC). The density functional theory (DFT) calculations served to obtain dissociation energies and reaction pathways, to elucidate the reaction mechanism. The oxidation of PI and THPI produced several toxic nitrogen-containing gases and volatile organic compounds, including hydrogen cyanide, isocyanic acid, nitrogen oxides, benzonitrile, maleimide and tentatively identified benzenemethanimine. The detection of dibenzo-*p*-dioxin (DD) and dibenzofuran (DF) suggests potential formation of the toxic persistent organic pollutants (POPs) in fires involving PI and THPI, in presence of a chlorine source. The oxidation of THPI produced 2-cyclohexen-1-one, a toxic unsaturated ketone. The results of the present study provide the data for quantitative risk assessments of emissions of toxicants in combustion processes involving PI and THPI.

1. Introduction

Phthalimide (PI) comprises an aromatic ring coupled to an imide moiety (Fig. 1). The compound itself and its derivatives are widely employed as feedstocks for manufacturing a number of industrial chemicals, primarily pesticides [1], polymer backbones [2,3] as well as plasticisers [4]. As an active component in the pigments production, PI is derivatised to make coloured units in the polymer dyes [5,6]. Tetrahydrophthalimide (THPI) constitutes an important derivative of PI, with the benzene ring replaced by a cyclohexene ring (Fig. 1). The application of THPI, as an intermediate for chemical synthesis, includes the productions of pesticides [7], polymers [8,9] and pharmaceuticals [10].

Large amounts of PI and THPI are frequently handled in manufacturing and storage facilities, owing to their numerous applications. Accidental chemical fires of PI and THPI may produce toxic substances, posing risks to people and the surrounding environment [11,12]. Sparse knowledge of the decomposition products of PI and THPI in fires necessitates urgent research. This situation is compounded by the fact that both PI and THPI constitute major products in the combustion of sulfenimide fungicides [13,14]. Furthermore, fire statistics have revealed a growing number of people injured or killed by inhaling toxic gases emitted in fires of polymers, as a consequence of increasing use of synthetic polymers and composites in construction and transport industries [15–17]. Polyimides and copolymers can break down into phthalimides [18,19], during their thermal decomposition, making a study of phthalimides themselves informative to evaluate the possible toxic products evolving in fires of polymers.

However, there is limited research on the thermal decomposition of PI and THPI, especially under conditions relevant to their decomposition in fires. Żurakowska-Orszàgh and Chreptowicz adopted PI as a simplified model to understand the loss of CO_2 during the thermal degradation of polyimides in an inert environment and reported the formation of toxic hydrogen cyanide [20]. So far, no efforts have been expanded to study the toxic gases from PI under oxidative conditions. Among chemicals structurally related to PI, the pyrolysis of acetylphthalimide has been examined between 220 and 325 °C [21]. The identified volatile products mainly arise from the acetyl group while the residual moiety leads to PI. However, the study included no further research on the decomposition of PI. Regarding the detailed research into the

* Corresponding author. Tel.: +61 2 4985 4433; fax: +61 2 4921 6893.
E-mail address: Bogdan.Dlugogorski@newcastle.edu.au (B.Z. Dlugogorski).
[1] Also at School of Chemistry, The University of Sydney.

0304-3894/$ – see front matter © 2011 Elsevier B.V. All rights reserved.
doi:10.1016/j.jhazmat.2011.01.040

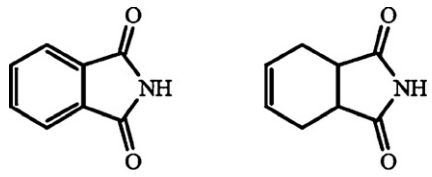

PI THPI

Fig. 1. Molecular structures of PI and THPI.

thermal behaviour of THPI, we attempted, unfortunately with no success, to locate any relevant literature.

This article constitutes an investigation into the vapour-phase thermal decomposition of PI and THPI, to determine the possible toxic pollutants at temperatures between 400 and 600 °C. An oxygen concentration of $6.0 \pm 0.5\%$ O_2 in N_2 (v/v) was employed for experiments under oxygen rich conditions while 280 ± 30 ppmv O_2 in N_2 (v/v) for the oxygen lean conditions, denoted hereafter as oxidation (OXD) and low oxygen pyrolysis (LOP), respectively. These two conditions resemble over-ventilated and under-ventilated combustion scenarios. The results of this study will facilitate assessments of the potential hazards posed by toxic products from combustion of PI or THPI to people and the surrounding environment.

2. Experimental methods

With details described elsewhere [22], the bench-scale apparatus (Fig. S1) consists of a fuel vaporiser, an isothermal alumina reactor and a collection system for different types of products. The gaseous products flow through a desiccant tube into a tedlar air-sampling bag for FTIR analysis. The volatile organic compounds (VOC) are captured, in separate experiments, by an adsorbent cartridge packed with 100 mg of activated charcoal while a glass tube loaded with two cartridges of silica gel (150 mg each) served to trap dibenzo-*p*-dioxin (DD) and dibenzofuran (DF). At the downstream end of the sampling line, we direct the exhaust gases through a chilled solvent trap (0 °C) which contains mixture of dichloromethane and methanol.

For the decomposition experiments, PI and THPI powders were loaded onto a tray in a polytetrafluoroethylene (PTFE) tube installed vertically inside a fuel vaporiser, with an old GC oven adapted for that purpose. To evaporate the two phthalimides at slow but comparable rates (approximately 0.046 mg min^{-1}), we maintained the oven at 140 °C for PI and 125 °C for THPI, respectively. The carrier gas was prepared by mixing controlled amounts of oxygen and nitrogen (both 99.999% pure). The fuel equivalence ratios (φ) in the LOP experiments corresponded to 13.6 and 15.9 for PI and THPI, respectively, close to pyrolysis conditions, while OXD experiments led to a very similar φ of 0.06 for PI and 0.07 for THPI. The decomposition of PI and THPI occurred in the central (reactor) zone of a high-temperature tube maintained by a three-zone electrically heated furnace. A transfer line (150 °C) coupled the reactor to the fuel vaporiser, with an adjustable alumina rod inserted into the reactor tube to maintain the same residence time of 1 s in all experiments.

The gaseous species collected into the sampling bag were diluted for a subsequent FTIR analysis, to maintain the signal intensity in the linear region (<0.7 absorbance unit) for all gases but CO_2. The QASoft software package provided a spectra library for the identification of gaseous products as well as a region integration and subtraction routine for quantitative analysis. Exceptionally, we quantified CO_2 by μGC because of its intense FTIR response. The activated charcoal cartridges were washed with 1 mL of carbon disulfide (CS_2) while the silica gel traps were extracted with 1 mL of acetone in an ultrasonic bath for 30 min. The use of a MS detector required the filtration of the extracts from washing the adsorbents prior to injecting the extracts into GC. Upon the conclusion of each run, we collected the products condensed inside the reactor with solvent for subsequent GC–MS analysis.

The infrared spectra were recorded on a Varian 660-IR spectrometer, fitted out with a 10 m permanently aligned long path gas cell. The GC–MS analyses were performed on a Varian CP3800 GC and Varian 1200 QMS, equipped with a 30 m Varian VF-5ms Factor-Four column (i.d. of 0.25 mm, film thickness of 0.25 μm). The results from repeated experiments suggested reasonable reproducibility. (See Supplementary Data, Section 2 for further details of analytical procedure, purity of chemicals, instrumental parameters and estimation of errors.)

3. Computational methods

The density functional theory (DFT) computations have been performed in order to obtain information on bond dissociation energies and reaction pathways, with detailed computation methods and theory levels outlined in Supplementary Data, Section 6.

4. Results and discussion

With the details of FTIR spectra interpreted in Supplementary Data (Fig. S2), the eight identified species under the oxidative conditions include isocyanic acid (HNCO), nitrogen monoxide (NO), nitrogen dioxide (NO_2), hydrogen cyanide (HCN), benzene (C_6H_6), 1,3-butadiene (C_4H_6) and carbon oxides (CO and CO_2). A number of studies have documented the negative effects of these nitrogen containing pollutants on health [23,24]. The yields of each pollutant were quantified as mole percent of initial reactant loading, with the yield-temperature profiles of N-containing gases displayed in Fig. 2.

The yields of HNCO from the oxidation of PI and THPI exhibit a similar trend, increasing to the corresponding maxima and then progressively decreasing to zero toward 600 °C. Less emission of HNCO was observed from PI compared to that from THPI. Nitrogen oxides exhibit increase in yields at elevated temperatures. The highest yield of NO from PI exceeds that of THPI, but a lesser amount of NO_2 was measured at 600 °C in the case of PI. The yields of HCN from the oxidation of two phthalimides increase with temperature up to 500 °C and decrease toward higher temperatures. Benzene and carbon oxides exhibit yields monotonically increasing with temperature in the oxidation of PI and THPI (Fig. S3). The analogous results were observed for carbon oxides, whereas THPI resulted in more benzene compared to PI, with yields of 2.1% and 1.0%, respectively at 600 °C.

Under the LOP conditions, we observed no N-containing gases produced from PI and THPI, with small amounts of carbon oxides arising from both phthalimides. The peak yields of CO and CO_2 from THPI correspond to 1.3% and 6.6%, respectively at 600 °C, higher than those from PI. The FTIR absorption of 1,3-butadiene was observed in the experiments involving THPI (>500 °C) only. The yield of 1,3-butadiene increased with temperature, achieving 58.7% at 600 °C.

The analyses of VOC identified benzonitrile (BZN), a toxic compound, as the only VOC product in the experiments of PI. Three VOC products were observed from THPI, with two of them identified as BZN and 2-cyclohexen-1-one (2-CHX). The latter is a toxic cyclic α,β-unsaturated ketone, reported as an environmental pollutant with mutagenic effects [25]. The tentative identification of the third product has been described elsewhere by matching its mass spectrum with the most likely structure (benzenemethanimine) in the NIST library [22], with no confirmation achieved owing to the lack of a commercially available standard. Fig. 3 illustrates the yield-

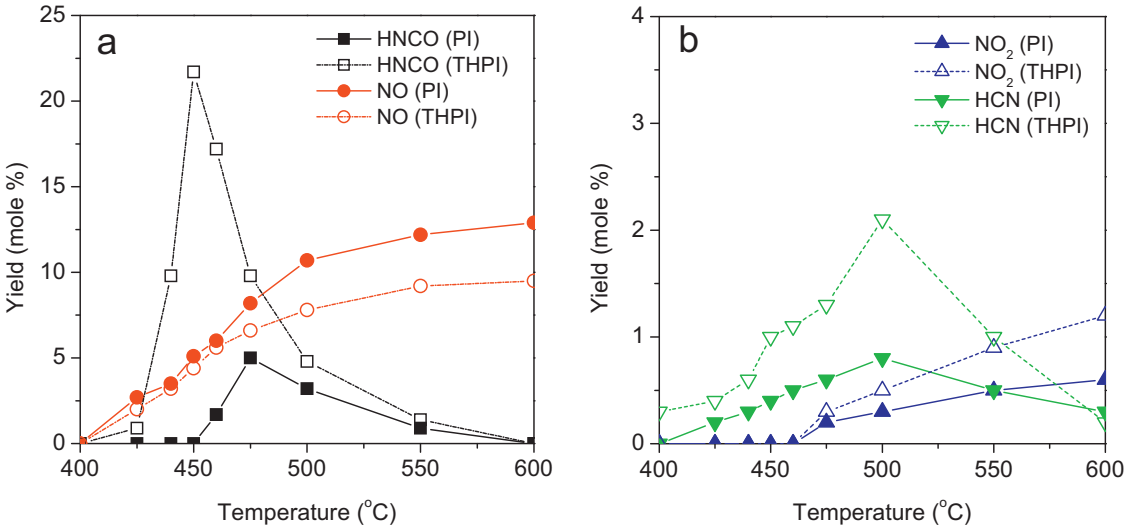

Fig. 2. Yield-temperature profiles of N-containing gases from the oxidation of PI and THPI; (a) HNCO and NO; (b) NO_2 and HCN.

temperature profiles of BZN, 2-CHX and the tentatively identified product (TIP) from PI and THPI. We assumed that TIP exhibits the same response factor as BZN on the MS detector and calculated approximate yields, to compare the trends.

The yields of BZN, in the oxidation of PI, increase with rising temperature, exhibiting a steep rise between 450 and 500 °C. Significantly lower yields of BZN were observed under the LOP conditions. Comparably, we observed a large amount of BZN from THPI under the OXD conditions, drastically exceeding those of LOP. Regarding the other two compounds arising from THPI, 2-CHX attains a maximum yield at 450 °C under the OXD conditions, with no detectable amount observed in the LOP experiments. The yields of TIP in both LOP and OXD experiments attain maxima between 450 and 500 °C, with steep declines as the temperature rises.

The chromatograms of condensed compounds indicated only one peak in the experiments of PI, with mass spectrum matched well with PI itself in the NIST library. However, the identification is challenged by one isomer of PI, *o*-cyanobenzoic acid. These two compounds exhibit indistinguishable mass spectra and elute at very close retention times, as indicated in the chromatogram. We have been able to confirm the identification of PI by the symmetric structure indicated by the Carbon-13 NMR spectrum (300 MHz), with details discussed elsewhere [22]. Under the OXD conditions, THPI resulted in two compound peaks, identified as PI and undecomposed THPI. The LOP experiment of THPI (>500 °C) resulted in the third condensed product, maleimide (MID), a corrosive and toxic compound [26]. Fig. 4 displays the yield-temperature profiles of condensed compounds (mole percent) and conversion of PI and THPI, respectively.

Under the OXD conditions, the complete conversion of PI occurs at 600 °C. However, a large portion of PI stays undecomposed at such temperature in the LOP experiments. Similarly, the overall decomposition of THPI proceeded significantly slower under the LOP conditions compared to the OXD results <500 °C. The lower oxygen concentration also reduced the conversion of THPI to PI, with the peak yield of PI corresponding to 13.8% (LOP) and 39.7% (OXD), respectively. The yield of maleimide increases up to 10.2% at 600 °C.

The yields of above products sum to a satisfactory carbon balance (>80%) for both PI and THPI, excluding the LOP experiments at high temperatures, where we observed the formation of soot. The deficiency of nitrogen in the oxidation experiments can be

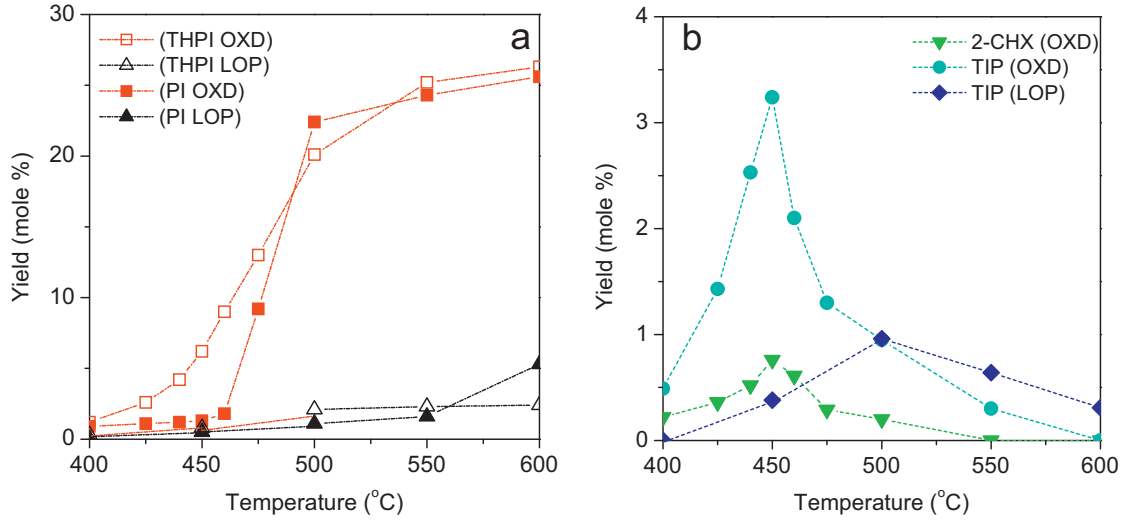

Fig. 3. Yield-temperature profiles of VOC products under both LOP and OXD conditions: (a) BZN from PI and THPI; (b) 2-CHX and TIP from THPI.

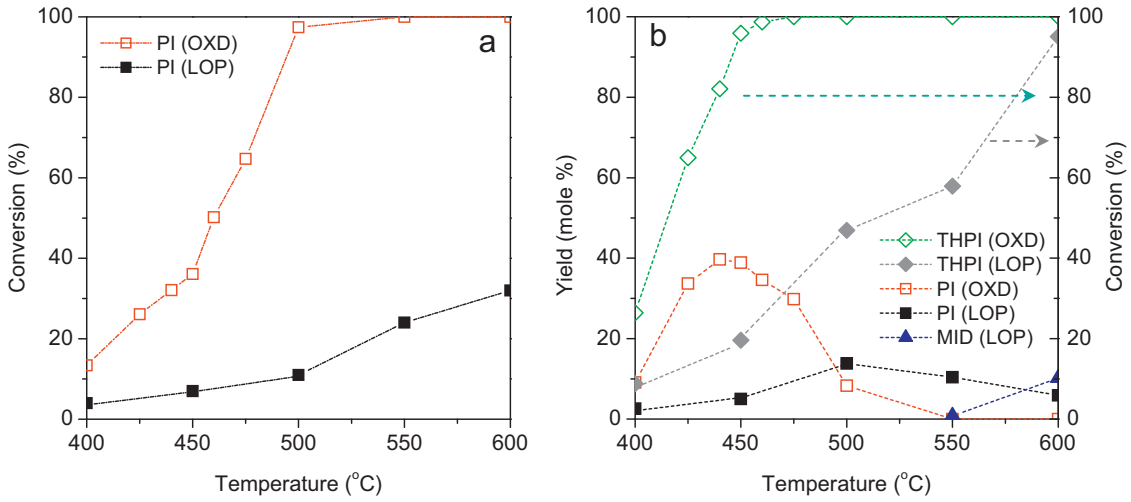

Fig. 4. Conversion of PI (a) and THPI (b) as well as and yield-temperature profiles of condensed species from THPI (b).

attributed to the formation of N_2, as evidenced by the experiments conducted under Ar/O_2 atmosphere [22]. Comparably, other oxidation studies of the N-containing materials documented N_2 as the dominant fate for the fuel-N and small yields of NO_x [27,28].

The yield distribution of DD/F in the sampling line of the oxidation experiments at 600 °C (see Table S4 for the detailed measurements) shows that the front silica gel cartridge trapped the dominant portion of DD/F. It also demonstrated an acceptable trapping efficiency in our experimental system, with no breakthrough into the solvent trap. The oxidation of both PI and THPI led to a higher yield of DF while THPI produced more DD/F than PI, with the yields of 38.3 ng DD and 5.1 ng DF per mg THPI compared to 15.1 ng DD and 3.3 ng DF per mg PI (Table S4). The formation of DD/F in decomposition of PI and THPI indicates that fires of phthalimides in the presence of a chlorine source may produce polychlorinated dibenzo-*p*-dioxins and dibenzofurans (PCDD/F). We have observed the formation of PCDD/F in a previous oxidation study of captan, a chlorinated fungicide with a THPI moiety [29].

The upper scheme in Fig. 5 illuminates a pyrolysis mechanism of PI suggested in the archival literature [20]. In a previous contribution, we have discussed that the decomposition of PI is not likely to proceed via these steps, owing to the incurred high energy barriers [22]. Instead, we have discovered another more favourable mechanism with lower energies (bottom in Fig. 5). The shift of H from N atom to O atom only requires 54 kcal mol^{-1} to reach a transition state (TS), resulting in an enol tautomer. After an isomerisation via a modest barrier of 11 kcal mol^{-1}, an additional 77 kcal mol^{-1} is needed to overcome the TS, which opens the five-member-ring to form benzoyl isocyanate (BIC). Subsequently, the loss of CO_2 can proceed with an energy barrier of 49 kcal mol^{-1}. However, limited formation of BZN can be expected under the O_2 free conditions given the relatively high intermediate barrier of 71 kcal mol^{-1}, as evidenced by the low yields of BZN under the LOP conditions. In comparison, the significantly higher yields of BZN under oxidation conditions point to the important role of O_2 which may facilitate the H shift from the OH group to the aromatic ring, reducing the energy needed to open the five-membered ring.

The experimental results suggest that the slow abstraction of H from the cyclohexene ring by O_2 dominates the initial stage of THPI decomposition. With further decomposition of PI restrained in the O_2 free environment, the overall decomposition of THPI under the LOP conditions is expectedly slower than under OXD. At higher temperature, the formation of 1,3-butadiene and maleimide indicates the rupture of the cyclohexene ring (on the left in Fig. 6a), takes place by a retro-Diels-Alder reaction [30]. Our quantum chemical calculations yield a barrier for the reaction leading to maleimide and *cis*-butadiene of 47 kcal mol^{-1}. At ambient temperature, *cis*-1,3-butadiene would convert into the more stable *trans*-1,3-butadiene [31].

Higher levels of O_2 under the OXD conditions facilitate the abstraction of H from the cyclohexene ring of THPI. Besides the complete aromatisation to PI, the abstraction of H may proceed via another route. The resulting 3a,7a-dihydrophthalimide-derived radical (R1) may induce a β-scission, opening the five-membered ring (right in Fig. 6a). We have located a TS for the resulting radical R2 to loose HNCO, requiring energy of 30.4 kcal mol^{-1} (left in Fig. 6b). Although HNCO was also detected in the oxidation of PI, significantly higher yields of HNCO were measured in the case of THPI. It confirms that β-scission can promote the formation of HNCO in the oxidation of THPI. Subsequently, the remaining part will decompose to CO and phenyl radical ($C_6H_5^{\bullet}$). Alternatively, the loss of CO prior to the ejection of HNCO from R2 radical may occur, with a slightly higher barrier. See Section 6 of Supplementary Data for the detailed calculations of the energetics of these two routes.

The decreasing yield of HNCO at elevated temperatures suggests that a further reaction consuming HNCO can occur in our experiments. As the radical pool builds up in the decomposition process, the abstraction of H would lead to NCO radical. The fast reaction between NCO and NO has been documented to form N_2 and CO_2 [32].

Benzonitrile was observed as a dominant VOC product arising from THPI decomposition, particularly at higher temperatures (Fig. 3a). The dramatic increase in BZN yield (>450 °C) was accompanied by the rapid decrease in the yield of PI, which suggests that, during the decomposition of THPI, the formation of BZN correlates to the decomposition of PI. Furthermore, with the five-membered ring opening by β-scission, the R2 radical can also give BIC by the expulsion of H, which should contribute the formation of BZN as well (on the right in Fig. 6b).

Benzene and HCN have been identified as important products of benzonitrile decomposition [33]. However, slightly higher peak yields of both species were observed in the oxidation of THPI while similar yields of benzonitrile were formed in the experiments on both phthalimides. Our previous calculations revealed that the abstraction of H from the cyclohexene ring of THPI can lead to the loss of further H from the cyclohexenyl or cyclohexedienyl derived radicals [14]. Tsang suggested that H can react with NCO radical to form HCN and O [34]. More NCO radicals can be expected in the oxidation of THPI, owing to the higher yield of HNCO. The reaction between NCO and available H source may explain the higher yield of

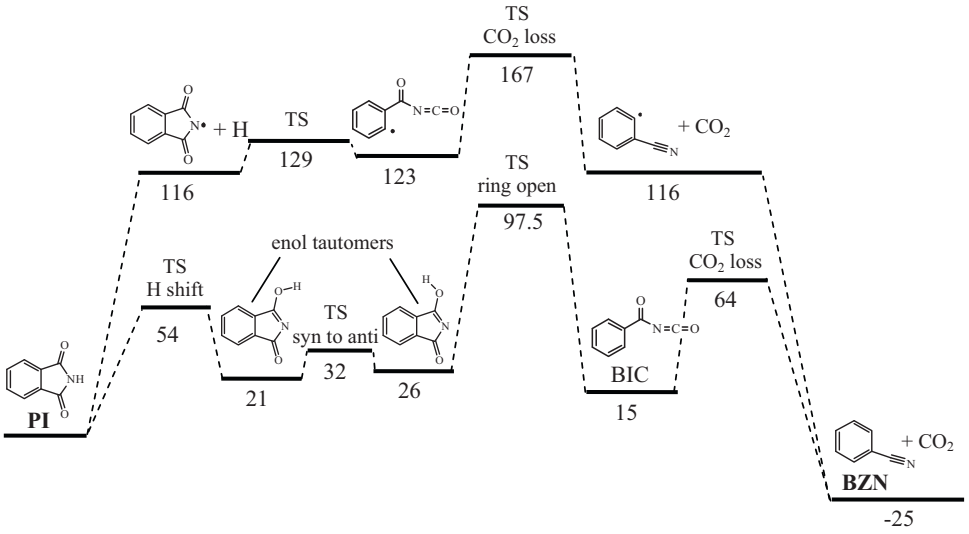

Fig. 5. Schematic profiles of potential energy surface for the decomposition of PI in inert atmosphere; note, numerical data correspond to the relative energies (in kcal mol^{-1}). Calculated at the B3LYP/6-311+G(3df,2p)//B3LYP/6-31G(d,p) level of theory.

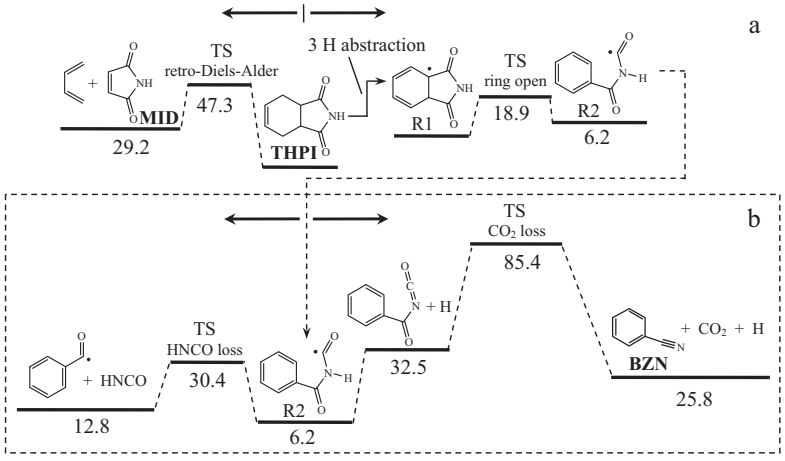

Fig. 6. Schematic profiles of potential energy surface for the decomposition of THPI; note, numerical data correspond to the relative energies (in kcal mol^{-1}). Calculated at the B3LYP/6-311+G(3df,2p)//B3LYP/6-31G(d,p) level of theory.

HCN from THPI than from PI. The loss of HNCO and CO from R2 radical leads to the formation of phenyl radical. Although most phenyl radicals will be oxidised, a small portion may recombine with H to form benzene. This process contributes to the higher yields of benzene from THPI compared to PI.

The reaction between phenyl radical and O_2 was reported to proceed through the formation of phenylperoxy radical [35]. Fission of the O–O bond gives phenoxy radical, which is a crucial intermediate in the formation of DD and DF in the oxidation of THPI and PI. The coupling of oxygen centred phenoxy radical to carbon centred phenoxy radical produces DD while the recombination between carbon centred phenoxy radical with itself or phenyl results in DF [36]. In comparison with the results of PI, the higher yields of DD and DF in the oxidation of THPI are consistent with the expected higher amounts of phenyl radicals and hence benzene in the case of THPI.

Regarding tentatively identified benzenemethanimine, there is a possibility that phenyl radical can react with HCN. Our previous quantum calculations [37] revealed that the exothermicity of this reaction amounts to 30.7 kcal mol^{-1} (0 K), with a barrier of only 4 kcal mol^{-1} (0 K). The resulting $C_6H_5CHN^{\bullet}$ radical recombines with H to form benzenemethanimine. Correspondingly, we observed higher yields of TIP from the oxidation of THPI than those of LOP, as the radical processes leading to phenyl and HCN are promoted under the OXD conditions. However, a high temperature would enable $C_6H_5CH=N^{\bullet}$ radical to overcome the TS for H loss of 31.4 kcal mol^{-1} to form BZN (Fig. S4). This proposition is consistent with the decreasing yields of TIP and increasing yields of BZN toward 600 °C observed in our experimentals. The detailed pathways from THPI to 2-CHX are somewhat uncertain. However, our quantum chemical calculations discovered pathways leading to 3-cyclohexen-1-one (3-CHX) which proceed via the β-scission of cyclohexenyl-derived radical (Fig. S5). We believe the further reaction involving 3-CHX in the oxidation process is crucial for the formation of 2-CHX.

5. Conclusions

In this contribution, the thermal decomposition of PI and THPI was investigated under oxidative conditions. Toxic products included a number of nitrogen containing gases (HNCO, NO_x and HCN), benzonitrile, maleimide and 2-cyclohexen-1-one. With 2-cyclohexen-1-one arising from THPI only, benzonitrile was identified as the major volatile organic product in both cases. The low oxygen pyrolysis of THPI formed toxic maleimide through the retro-Diels-Alder reaction of its cyclohexene ring. The oxidations of PI

and THPI also led to the formation of nonchlorinated DD/F, pointing to the propensity of producing PCDD/F when they are burnt in the presence of a source of chlorine. Combined with our quantum chemical calculations, the yields of these products were compared between THPI and PI. In addition to the quantitative information on the toxic products from the combustion of these two phthalimide compounds, this study also proposed the decomposition pathways leading to toxic species. H abstraction from the cyclohexene ring of THPI can induce β-scission, resulting in the rupture of the C–C bond between the ring and carbonyl group, which contributes to the difference in the yields of products from the oxidation of PI and THPI.

Acknowledgements

This study has been funded by the Australian Research Council (Project No. DP0988907). We acknowledge with gratitude discussions with Dr Ian Van Altena from the Department of Chemistry, The University of Newcastle (Australia) on NMR identification and Professor Adam Grochowalski of the Cracow Technical University (Poland) on analytical methodologies.

Appendix A. Supplementary data

Supplementary data associated with this article can be found, in the online version, at doi:10.1016/j.jhazmat.2011.01.040.

References

[1] P.E. Russell, A century of fungicide evolution, J. Agric. Sci. 143 (2005) 11–25.
[2] Z. Peng, L. Yu, Second-order nonlinear optical polyimide with high-temperature stability, Macromolecules 27 (1994) 2638–2640.
[3] X. Guo, F.S. Kim, S.A. Jenekhe, M.D. Watson, Phthalimide-based polymers for high performance organic thin-film transistors, J. Am. Chem. Soc. 131 (2009) 7206–7207.
[4] M. Ash, I. Ash, Handbook of Preservatives, Synapse Information Resources Inc., New York, 2004.
[5] J.A. Simms, A new graft polymer pigment dispersant synthesis, Prog. Org. Coat. 35 (1999) 205–214.
[6] F. Dierschke, J. Jacob, K. Müllen, A hybrid polymer of polyaniline and phthalimide dyes, Synth. Met. 156 (2006) 433–443.
[7] A.R. Kittleson, Fungicides, preparation and some properties of *N*-trichloromethylthiotetrahydrophthalimide, J. Agric. Food Chem. 1 (1953) 677–679.
[8] V. Bounor-Legare, P. Mison, B. Sillion, Thermal reaction of *N*-(4′-benzyl)phenyl-1,2,3,6-tetrahydrophthalimide: a model for the behaviour of tetrahydrophthalimide end-capped oligomers, Polymer 39 (1998) 2825–2833.
[9] V. Gaina, C. Gaina, Synthesis and characterization of poly(ester-urethane-imide)s by Diels-Alder polyaddition, Polym. Plast. Technol. Eng. 41 (2002) 523–540.
[10] Z. Mikhail, S. Timothy, G.K.S. Prakash, A.K. Mikhail, *N*-Amino-exo-3,6-epoxy-1,2,3,6-tetrahydrophthalimide as an active aminoaziridinating agent, Eur. J. Org. Chem. 2009 (2009) 3635–3642.
[11] F. Markert, Assessment and mitigation of the consequences of fires in chemical warehouses, Saf. Sci. 30 (1998) 33–44.
[12] P. Kinsman, T.E. Maddison, Hazard assessment for fires in agrochemical warehouses: the role of combustion products, Process Saf. Environ. Prot. 79 (2001) 145–156.
[13] W. Klusmeier, K.H. Ohrbach, P. Kühn, A. Kettrup, Investigations into the thermal decomposition of selected pesticides, J. Anal. Appl. Pyrolysis 16 (1989) 205–211.
[14] K. Chen, J.C. Mackie, E.M. Kennedy, B.Z. Dlugogorski, Thermal decomposition of captan and formation pathways of toxic air pollutants, Environ. Sci. Technol. 44 (2010) 4149–4154.
[15] Office of the Deputy Prime Minister, Fire Statistics United Kingdom 2004, Office of the Deputy Prime Minister, London, 2006.
[16] D.A. Purser, The performance of fire retardants in relation to toxicity, toxic hazard and risk in fires, in: A.R. Horrocks, D. Price (Eds.), Fire Retardant Materials, CRC Press/Woodhead Publishing, Cambridge, UK, 2001.
[17] A.A. Stec, T.R. Hull, K. Lebek, Characterisation of the steady state tube furnace (ISO TS 19700) for fire toxicity assessment, Polym. Degrad. Stab. 93 (2008) 2058–2065.
[18] C. Sabrina, P. Concetto, M. Giorgio, Thermal degradation mechanisms of polyetherimide investigated by direct pyrolysis mass spectrometry, Macromol. Chem. Phys. 200 (1999) 2345–2355.
[19] M.F. Coskun, K. Demirelli, M. Coskun, M. Dogru, Thermal decomposition of poly[3-phthalimido-2-hydroxypropyl methacrylate], Polym. Degrad. Stab. 76 (2002) 145–154.
[20] J. Żurakowska-Orszàgh, T. Chreptowicz, Thermal degradation of polyimides—II: mechanism of carbon dioxide formation during thermal degradation, Eur. Polym. J. 17 (1981) 877–880.
[21] C.D. Hurd, M.F. Dull, J.W. Williams, The decomposition of acetylphthalimide, J. Am. Chem. Soc. 57 (1935) 774–775.
[22] K. Chen, D. Wojtalewicz, J.C. Mackie, E.M. Kennedy, B.Z. Dlugogorski, Hazardous air pollutants formed in fires of phthalimide compounds, in: Proceedings of 8th Asia-Oceania Symposium on Fire Science and Technology, Victoria University, Melbourne, in press.
[23] M. Boutin, A. Dufresne, C. Ostiguy, J. Lesage, Determination of airborne isocyanates generated during the thermal degradation of car paint in body repair shops, Ann. Occup. Hyg. 50 (2006) 385–393.
[24] K.T. Paul, T.R. Hull, K. Lebek, A.A. Stec, Fire smoke toxicity: the effect of nitrogen oxides, Fire Saf. J. 43 (2008) 243–251.
[25] M.L. Cunningham, H.C. Price, R.W. O'Connor, M.P. Moorman, J.F. Mahler, J.B. Nold, D.L. Morgan, Inhalation toxicity studies of the α,β-unsaturated ketones:2-cyclohexene-1-one, Inhal. Toxicol. 13 (2001) 25–36.
[26] U. Yosh Imasa, J.M. Fisher, M. Rabinovitz, Showdomycin and its reactive moiety, maleimide: a comparison in selective toxicity and mechanism of action in vitro, Biochem. Pharmacol. 29 (1980) 2199–2204.
[27] D.A. Purser, J.A. Purser, HCN yields and fate of fuel nitrogen for materials under different combustion conditions in the ISO 19700 tube furnace, in: Proceedings of 9th International Symposium, International Association for Fire Safety Science, University of Karlsruhe, Germany, 2008, pp. 1117–1128.
[28] P.M. Nicholls, P.F. Nelson, Detection of HNCO during the low-temperature combustion of coal chars, Energy Fuel 14 (2000) 943–944.
[29] K. Chen, D. Wojtalewicz, M. Altarawneh, J.C. Mackie, E.M. Kennedy, B.Z. Dlugogorski, Formation of polychlorinated dibenzo-*p*-dioxins and dibenzofurans (PCDD/F) in oxidation of captan pesticide, Proc. Combust. Inst. 33 (2011) 701–708.
[30] D.K. Lewis, D.A. Glenar, S.M. Hughes, B.L. Kalra, J. Schlier, R.J. Shukla, J.E. Baldwin, Stereochemistry of the retro Diels-Alder reaction of *cis*,exo-5,6-d2-bicyclo[2.2.2]oct-2-ene, Abstr. Pap. Am. Chem. Soc. 221 (2001) 355.
[31] J.E. Rice, B. Liu, T.J. Lee, C. McMichael Rohlfing, The structure of *cis*-butadiene, Chem. Phys. Lett. 161 (1989) 277–284.
[32] P. Glarborg, J.A. Miller, Mechanism and modeling of hydrogen cyanide oxidation in a flow reactor, Combust. Flame 99 (1994) 475–483.
[33] S-.T. Etemad-Rad, E. Metcalfe, The pyrolysis of benzonitrile, Fire Mater. 17 (1993) 33–37.
[34] W. Tsang, Chemical kinetic data-base for propellant combustion—reactions involving CN, NCO, and HNCO, J. Phys. Chem. Ref. Data 21 (1992) 753–791.
[35] G. da Silva, J.W. Bozzelli, Variational analysis of the phenyl + O_2 and phenoxy plus O reactions, J. Phys. Chem. 112(A) (2008) 3566–3575.
[36] I. Wiater, J.G.P. Born, R. Louw, Products, rates, and mechanism of the gas-phase condensation of phenoxy radicals between 500–840 K, Eur. J. Org. Chem. (2000) 921–928.
[37] K. Chen, J.C. Mackie, E.M. Kennedy, B.Z. Dlugogorski, Air pollutants formed in thermal decomposition of folpet fungicide under oxidative conditions, Environ. Sci. Technol. 45 (2011) 554–560.